LETTERS
PUBLISHED ONLINE: 31 OCTOBER 2010 | DOI: 10.1038/NGEO990
nature geoscience

Silica deposits in the Nili Patera caldera on the Syrtis Major volcanic complex on Mars

J. R. Skok[1]*, J. F. Mustard[1], B. L. Ehlmann[1], R. E. Milliken[2] and S. L. Murchie[3]

The martian surface features abundant volcanoes and evidence for past liquid water. Extant or relict martian volcanic hydrothermal systems have therefore been sought in the pursuit of evidence for habitable environments[1]. The Mars Exploration Rover, Spirit, detected deposits highly enriched in silica with accessory minerals, suggesting formation by hydrothermal leaching of basaltic rocks by low-pH solutions[2]. However, extensive erosion has obscured the context of the formation environment of these deposits. Silica deposits have also been identified remotely, but also with limited contextual clues to their formation; aqueous alteration products of basalt and volcanic ash are the most likely sources[3,4]. Here we report the detection from orbit of hydrated silica deposits on the flanks of a volcanic cone in the martian Syrtis Major caldera complex. Near-infrared observations show dozens of localized hydrated silica deposits. As a result of the morphology of these deposits and their location in and around the cone summit, we suggest that the deposits were produced by a volcanically driven hydrothermal system. The cone and associated lava flows post-date Early Hesperian volcano formation. We conclude that, if a relict hydrothermal system was associated with the silica deposits, it may preserve one of the most recent habitable microenvironments on Mars.

The Syrtis Major volcanic complex is a type example of Hesperian-aged plains volcanism on Mars. Crater statistics indicate that the complex was formed in the Early Hesperian period with major resurfacing completed by ~3.7 Gyr ago[5]. Orbital observations at thermal infrared and visible and near-infrared wavelengths constrain the modal mineralogy and show the rocks to be consistent with an olivine-bearing basaltic lava enriched in high-calcium pyroxene[6,7]. Near the centre of Syrtis Major are two named calderas, Nili Patera and Meroe Patera, at the northern and southern ends of an elongated depression that may result from multiple episodes of caldera formation[5,8]. The Nili Patera caldera (Fig. 1) hosts a 100-m-high degraded cone on the northeastern side of its floor, and a related lighter-toned lava flow to the west of the cone. The Nili Patera volcanic cone (Fig. 2) is unique in its region and is the only local late-stage volcanic feature with significant topography, possibly indicating a relatively viscous lava composition. Thermal infrared spectral properties of the flow have been interpreted as due either to a glassy dacitic composition or possibly a high-Si glass alteration product[9]. The west flank of the cone exhibits a moderate slope with surface streaks probably formed by downslope movement of unconsolidated material. The east flank seems to have been removed, possibly by explosive eruptive processes or extensive erosion.

Recent observations of the volcanic cone and associated lava flow by the Compact Reconnaissance Imaging Spectrometer

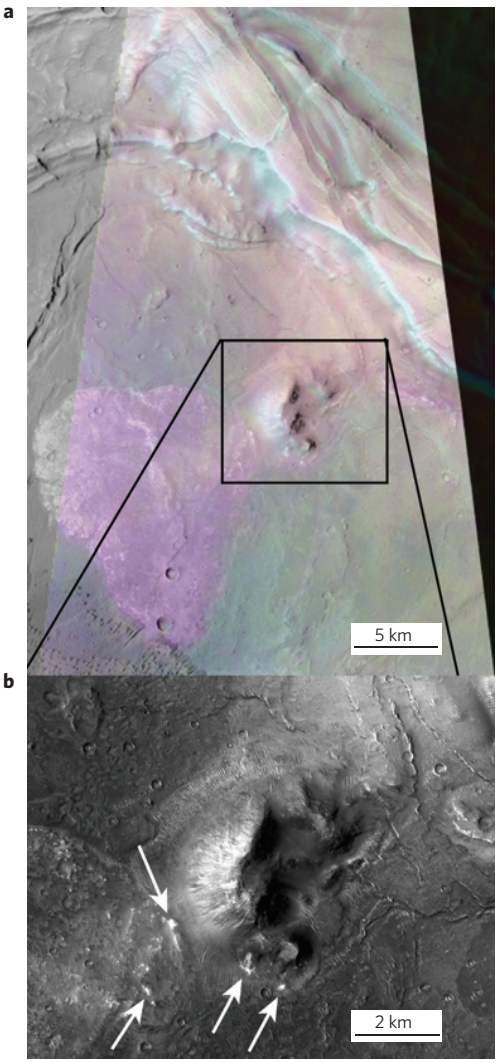

Figure 1 | Image of the Nili Patera caldera in Syrtis Major. a, CTX greyscale imagery overlain with a decorrelation stretch of Thermal Emission Imaging System (THEMIS) bands 9, 7 and 5. The pink regions correspond with Si-enriched areas as indicated by deconvolution of Thermal Emission Spectrometer spectra[9]. **b**, Cone structure; arrows indicate the largest of the deposits discussed in this Letter. However, all of the bright areas to the left of the arrows exhibit similar spectral features if they are large enough to fill a CRISM pixel. (CTX: P04_002427_1888_XI_08N292W; THEMIS: I09472026 (ref. 30)).

[1]Department of Geological Sciences, Box 1846, Brown University, Providence, Rhode Island 02912, USA, [2]Department of Civil Engineering and Geological Sciences, University of Notre Dame, Notre Dame, Indiana 46556, USA, [3]John Hopkins University, Applied Physics Laboratory, Laurel, Maryland 20723, USA. *e-mail: john_skok@brown.edu.

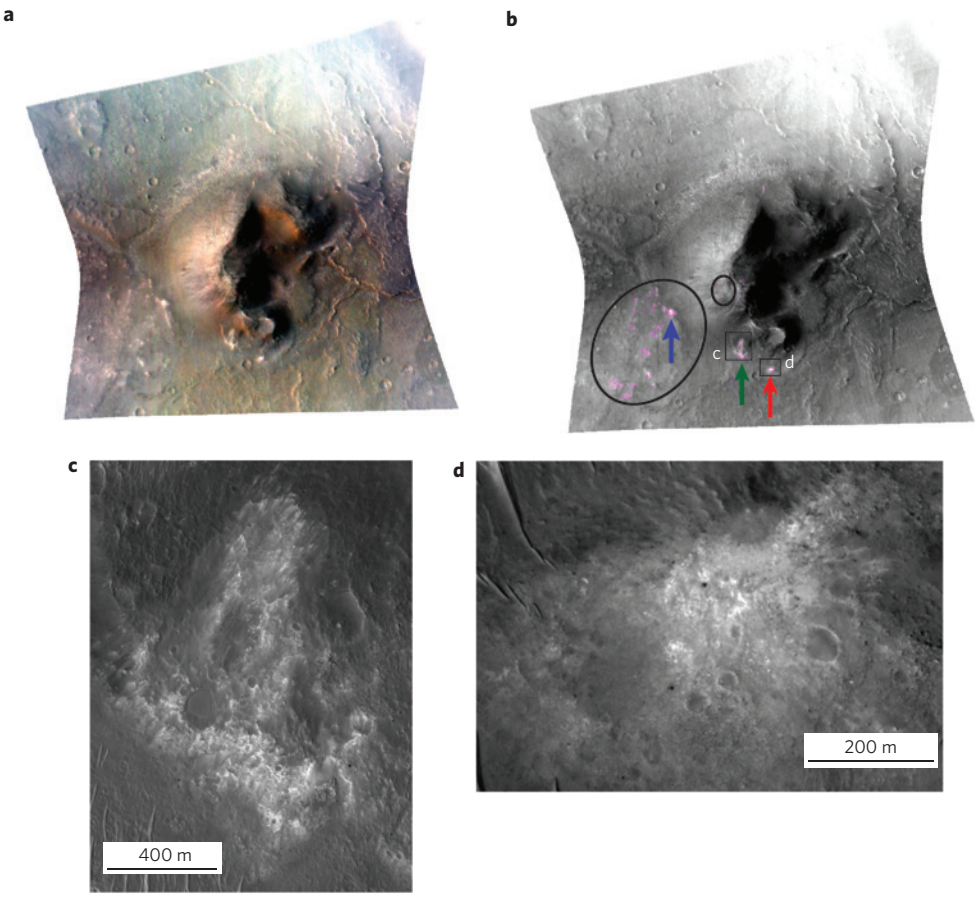

Figure 2 | CRISM and HiRISE observations of silica deposits. a, CRISM red–green–blue composite (red: 2.4 μm, green: 1.5 μm, blue: 1.1 μm) of the Nili Patera cone with deposits (image FRT00010628). The CRISM images are ~10 km across at the centre. **b**, Custom 2.2 μm band depth map with magenta indicating detections. The large black ellipse indicates a large field with many discrete deposits; the small black ellipse indicates summit deposits. The blue, green and red arrows correspond to the deposit spectra shown in Fig. 3. **c**, HiRISE image of a flank deposit showing a fan shape. **d**, HiRISE image of a floor deposit to the south of the cone showing a typical semicircular shape (HiRISE: ESP_013582_1895).

for Mars (CRISM) on the Mars Reconnaissance Orbiter (MRO) show that many of the small exposures of light-toned materials exhibit distinct spectroscopic signatures consistent with hydrated silica. Although silica has been detected at several other locations on Mars[2–4], this is its first detection in association with an intact volcanic source, providing a clear contextual link between mineralogy and morphology.

The deposits identified on and around the Nili Patera cone are characterized by a deep, broad asymmetric absorption near 2.2 μm (Fig. 3). The band depth of this feature is 3–4% and the exact band centre shifts from 2.21 to 2.25 μm depending on the particular deposit. Spectral ratios of the light-toned deposits also exhibit enhancement of a broad absorption centred near 3 μm. Large-area spectral averages show 1.4- and 1.9 μm absorptions that are just detectable above the level of noise in the data (for example, the 1.9 μm absorption in Fig. 3c).

A broad absorption near 2.21 μm is caused by a combination vibrational absorption (OH stretch and Si–OH bend) that produces overlapping absorptions at 2.21 μm and 2.26 μm caused by isolated Si–OH and H-bound Si–OH, respectively[10,11]. These are distinct from narrower Al–OH features near 2.2 μm in aluminium-bearing phyllosilicates[3]. In silica samples, a broad absorption band near 3.0 μm is related to the fundamental OH^- stretching vibrations, H_2O features at 2.8–2.9 μm due to symmetric and asymmetric stretches, and the ~3.1 μm overtone of the H_2O bending vibration[11]. Laboratory silica samples also typically exhibit absorption features near 1.4 μm due to the OH-stretch overtone near 1.38–1.39 μm and H_2O overtones from 1.41 to 1.46 μm (refs 10,11) as well as a 1.9 μm H_2O combination (bend plus stretch) vibration[12].

The Nili Patera detections are spectrally distinctive from detections of opaline silica and a similar broad 2.2 μm absorption elsewhere on Mars because of their comparatively weak 1.4- and 1.9 μm hydroxyl- and H_2O-related absorption features[11]. Laboratory experiments have shown that dehydration of silica can decrease the strength of H_2O-related absorptions through either heating[3,12] or exposure to a Mars analogue atmosphere[13]. Additional constituents in the deposits such as iron oxides, could obscure the shorter wavelength vibrational absorptions and may also be responsible for the enhanced short-wavelength (<1.5 μm) broad absorption in non-ratioed spectra[12] (Fig. 3c). Fe oxides and Ti oxides have been shown to co-occur with hydrated silica precipitates in terrestrial settings as micrometre-scale coatings[14–16]. The asymmetrical shape, strength, width and position of the 2.21 μm absorption, the presence of an enhanced 3 μm feature and the weak presence of the 1.4- and 1.9 μm absorptions all support identification of weakly hydrated amorphous silica (for example, H_2O-poor opal-A) as the spectrally distinct phase. However, it is important to note that from the present spectral observations we cannot conclusively determine whether this deposit represents typical hydrated silica that subsequently lost much of the adsorbed H_2O, whether the distinctive spectral properties represent an original characteristic of these silica deposits, or whether the hydration features are merely being obscured by other constituents.

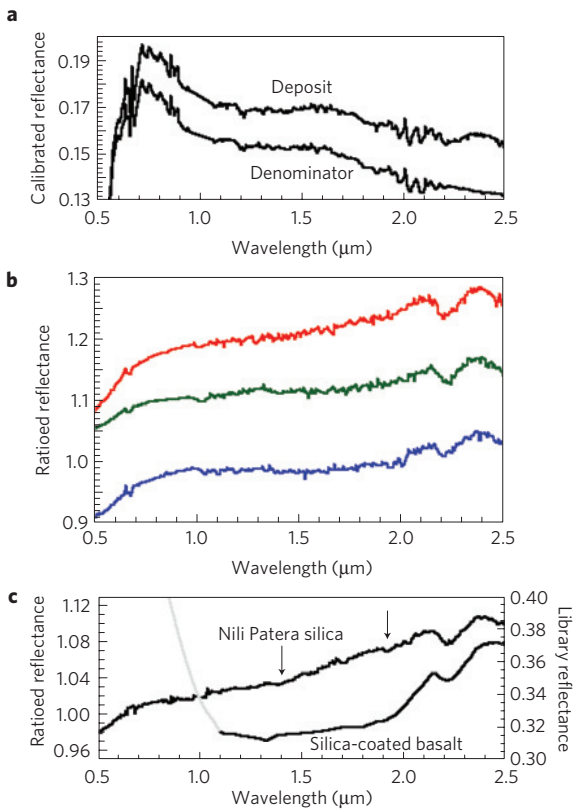

Figure 3 | Mineral deposit spectra indicative of Si–OH. a, Calibrated spectra of the unit indicated by the red arrow in Fig. 2b and the corresponding denominator spectra. The most distinctive feature is the absorption band at 2.2 μm. **b**, Ratioed spectra from the regions indicated by the coloured arrows in Fig. 2. Detection is based on the characteristic absorption at 2.2 μm. **c**, Average ratioed spectra from regions of interest that include all bright deposits (magenta in Fig. 2b). The arrows indicate possible weak water absorptions at 1.4 and 1.9 μm. A laboratory spectrum of silica-coated basalt is shown for comparison[15]. Note the similar 2.2 μm Si–OH absorption. The strong increase in reflectance of the library sample at low wavelengths is due to the presence of Fe^{3+} not seen in the Mars data.

The distribution of silica was mapped on the basis of the strengths of combination absorptions using spectral parameters[17] (see Methods; Fig. 2). The parameters highlight regions of interest that are then validated by examination of spectra. For the Nili Patera cone, the spectral parameter map of the 2.2 μm combination tone correlates to light-toned surface deposits.

The silica deposits are located on the lower section of the southwest side of the cone and are associated with the light-toned flow to the south and west of the cone and near the cone's summit (Fig. 2a,b). These silica-bearing deposits are limited to the region immediately near the volcanic cone. Detection of the diagnostic 2.21 μm spectral feature is equivocal in light-toned deposits located at the far western edge of the light-toned volcanic flow.

The silica deposits range in area from 0.14 km^2 to the 18 m per pixel resolution of the CRISM instrument. The largest deposit is on the western flank of the cone, and radiates from a high point at 290 m elevation in a fan shape down to the cone base at 230 m. High-Resolution Imaging Science Experiment (HiRISE) imagery of this deposit at 30 cm per pixel (Fig. 2c) indicates that the silica is in a diffuse deposit mixed with mobile surface material that preferentially fills in the topographic lows. As a result of the location and morphology of this cone-flank silica deposit, we infer that it preserves the original setting of silica formation, although present observations cannot determine whether the fan shape of the deposit results from the precipitation of silica from surface fluid flows or from erosion of a buried deposit. The silica deposits located on the light-toned volcanic flow on the floor of the Nili Patera caldera are smaller and are circular or semicircular in shape, possibly indicating localized source vents (Fig. 2d). Additional silica deposits occurring west of the cone's summit ridge are exposed in several constant elevation layers, with just a thin band visible among the volcanic slope debris.

The formation of silica has been extensively studied in a wide variety of environments on Earth. Silica sinter precipitated from fluids is associated with hydrothermal systems[18,19], but aerially extensive regions with silica can also be produced by acid-fog alteration[20] or as alteration products from the weathering of ash or volcanic materials[21]. Many of these scenarios have been considered for martian environments[22,23] and we describe the various mechanisms in terms of the Nili Patera geologic context.

The first formation mechanism considered is that silica-rich precipitate is deposited as acidic, volcanically driven ground waters leach Si from the basaltic substrate and become Si-saturated[24]. When this water reaches the surface, or near-surface, it deposits the silica in a hot spring environment. This scenario would require the presence of subsurface groundwater in Nili Patera during plutonic activity and deposit formation. The presence of silica deposits near the summit of the cone argues against this mechanism being solely responsible for the deposits, owing to the lack of a groundwater source.

A second scenario is that the cone and associated Si-rich flow are the result of an evolved magma chamber with a high Si content. Magmatic waters concentrated by fractionation and saturated with silica could rise in steam vents forming fumaroles and hot springs on the flanks and terrain local to the cone[25]. Subsequent precipitation of silica near the vents could lead to the observed deposits. This scenario requires internal plutonic fractionation to concentrate mantle water abundances and produce high Si compositions. It is also possible that some combination of magmatic waters, ground water and basaltic leaching led to the deposit formation, explaining the presence of deposits at all elevations.

In addition to these high-temperature formation mechanisms, silica deposits can be formed by low-temperature processes. Prominent among these is acid-fog alteration that dissolves the oxide components of the basaltic surface and precipitates amorphous silica[25]. This process can potentially affect the large areas seen in Nili Patera, but we observe only localized silica deposits. This process commonly deposits jarosite and other sulphate minerals[26] that have not yet been detected, although lack of orbital detection is not conclusive of their absence.

Given the silica spectral detections coupled with the volcanic context, we propose that high-temperature hydrothermal processes formed these silica deposits. In addition, the insolubility of Si in vapour[27] that limits the deposition of silica from a Si-saturated cloud requires either precipitation from a surface liquid or *in situ* surface alteration (for example, by acid fog). However, the apparent monomineralic composition of the detected alteration phases, their position on the volcanic cone and the spatial distribution of the deposit are best explained by a volcanically driven hydrothermal system. This system would have been active during the latest stages of post-Noachain Syrtis Major volcanism, possibly with an internally derived water source formed in a differentiated magma body.

Formation of the Syrtis Major caldera and Nili and Meroe pateras post-date the emplacement of the Syrtis Major volcanics in the Early Hesperian, and the formation of Meroe Patera has been dated to the Early Hesperian[5]. The formation of the dacite flow and the Nili Patera silica deposits are both interpreted to

result from late-stage volcanism within the Syrtis Major complex, and to be among the most recent deposits of hydrated minerals detectable from Mars orbit. Similar hydrothermal environments of silica formation on Earth often fossilize microbial life and silica deposits are considered to have a significant potential for preserving microbial fossils[1]. With clear volcanic context and post-Early Hesperian age, these remnant hydrothermal deposits may represent an aqueous environment on Mars that was both habitable and conducive to preservation.

Methods

Observations from the CRISM instrument provide the visible/near-infrared spectroscopic signatures of these cone deposits that were used to make the alteration mineral detection. The CRISM imaging spectrometer measures solar reflectance in the visible and near-infrared wavelength region (0.36–3.92 μm) with a full spatial resolution of ~18 m per pixel (ref. 28). CRISM data are calibrated to radiance and divided by the solar spectrum, giving values of the ratio of radiance to incident solar radiation (I/F) values. Simple photometric and atmospheric corrections are then carried out on a pixel-by-pixel basis by first dividing by the cosine of the incidence angle and then dividing by a scaled atmospheric transmission spectrum obtained using the 'volcano scan' method[22]. The volcano scan corrects for attenuation by atmospheric gases by dividing out gas absorptions measured empirically, using a ratio of plains adjacent to the summit of Olympus Mons. Initial mineral detections were made with the following custom parameter that was developed to compensate for the signal-to-noise level and highlight the featured deposits: $1 - 2.0 \times b1/(b2 + b3)$, where b1 is the average of 10 bands ranging from 2.19 to 2.25 μm, b2 is the average of 10 bands ranging from 2.05 to 2.13 μm and b3 is the average of 10 bands ranging from 2.36 to 2.43 μm.

Morphological analysis of regional and local geology was carried out with images from MRO's HiRISE (ref. 23) and Context Camera[29] (CTX).

Received 10 June 2010; accepted 24 September 2010; published online 31 October 2010

References

1. Farmer, J. D. & Des Marais, D. J. Exploring for a record of ancient Martian life. *J. Geophys. Res.* **104,** 26977–26995 (1999).
2. Squyres, S. W. *et al.* Detection of silica-rich deposits on Mars. *Science* **320,** 1063–1067 (2008).
3. Milliken, R. E. *et al.* Opaline silica in young deposits on Mars. *Geology* **36,** 847–850 (2008).
4. Ehlmann, B. L. *et al.* Identification of hydrated silicate minerals on Mars using MRO-CRISM: Geologic context near Nili Fossae and implication for aqueous alteration. *J. Geophys. Res.* **114,** E00D08 (2009).
5. Hiesinger, H. & Head, J. W. III The Syrtis Major volcanic province, Mars: Synthesis from Mars global surveyor data. *J. Geophys. Res.* **109,** E01004 (2004).
6. Mustard, J. F., Murchie, S. M., Erard, S. & Sunshine, J. *In situ* compositions of Martian volcanics: Implications for the mantle. *J. Geophys. Res.* **102,** 25605–25615 (1997).
7. Rogers, A. D. & Christensen, P. R. Surface mineralogy of Martian low-albedo regions from MGS-TES data: Implications for upper crustal evolution and surface alteration. *J. Geophys. Res.* **112,** E01003 (2007).
8. Crumpler, L. S., Head, J. W. & Aubele, J. C. Calderas on Mars: Characteristics, structure, and associated flank deformation. *Geol. Soc. Spec. Pub.* **110,** 307–348 (1996).
9. Christensen, P. R. *et al.* Evidence for magmatic evolution and diversity on Mars from infrared observations. *Nature* **436,** 504–509 (2005).
10. Anderson, J. H. Jr & Wickersheim, K. A. Near infrared characterization of water and hydroxyl groups on silica surfaces. *Surf. Sci.* **2,** 252–260 (1964).
11. Goryniuk, M. C., Rivard, B. A. & Jones, B. The reflectance spectra of opal-A (0.5–25 μm) from the Taupo volcanic zone: Spectra that may identify hydrothermal systems on planetary surfaces. *Geophys. Res. Lett.* **31,** L24701 (2004).
12. Milliken, R. E. PhD dissertation, Brown Univ. (2006).
13. Rice, M. S., Cloutis, E. A. & Crowley, J. K. Spectral reflectance changes accompanying long-duration exposure of silica sinter and Fe-sulfates to simulated Mars surface conditions. *Abstr. Lunar Planet. Conf.* 2576 (2010).
14. Sherman, D. M., Burns, R. G. & Burns, V. M. Spectral characteristics of the iron oxides with applications to the Martian bright region mineralogy. *J. Geophys. Res.* **87,** 10169–10180 (1982).
15. Chemtob, S. M., Jolliff, B. L., Rossman, G. R., Eiler, J. M. & Arvidson, R. E. Silica coatings in the Ka'u Desert, Hawaii, a Mars analog terrain: A micromorphogical, spectral, chemical and isotopic study. *J. Geophys. Res.* **115,** E04001 (2009).
16. Seelos, K. D. *et al.* Silica in a Mars analog environment: Ka'u Desert, Kilauea Volcano, Hawaii. *J. Geophys. Res.* **115,** E00D15 (2010).
17. Pelkey, S. M. *et al.* CRISM multispectral summary products: Parameterizing mineral diversity on Mars from reflectance. *J. Geophys. Res.* **112,** E08S14 (2007).
18. Rodgers, K. A. *et al.* Silica phases in sinters and residues form geothermal fields of New Zealand. *Earth Sci. Rev.* **66,** 1–61 (2004).
19. Preston, L. J., Benedix, G. K., Genge, M. J. & Sephton, M. A. A multidisciplinary study of silica sinter deposits with applications to silica identification and detection of fossil life on Mars. *Icarus* **198,** 331–350 (2008).
20. Schiffman, P., Zierenberg, R., Marks, N., Bishop, J. L. & Dyar, M. D. *et al.* Acid-fog deposition at Kilauea volcano: A possible mechanism for the formation of siliceous-sulfate rock coatings on Mars. *Geology* **34,** 921–924 (2006).
21. McLennan, S. M. Sedimentary silica on Mars. *Geology* **31,** 315–318 (2003).
22. Mustard, J. F. *et al.* Composition, morphology, and stratigraphy of Noachian crust around the Isidis basin. *J. Geophys. Res.* **114,** E00D12 (2009).
23. McEwen, A. S. *et al.* Mars Reconnaissance Orbiter's High Resolution Imaging Science Experiment (HiRISE). *J. Geophys. Res.* **112,** E05S02 (2007).
24. Morris, R. V. *et al.* The hydrothermal system at Home Plate in Gusev crater, Mars: Formation of high silica material by acid-sulfate alteration of basalt. *Abstr. Lunar Planet. Conf.* 2208 (2008).
25. Ruff, S. W. *et al.* The nature and distribution of silica at Home Plate in Gusev crater, Mars: Evidence for a hydrothermal system. *Abstr. Lunar Planet. Conf.* 2213 (2008).
26. Tosca, N. J., McLennan, S. M., Lindsley, D. H. & Schoonen, M. A. A. Acid-sulfate weathering of synthetic Martian basalt: The acid fog model revisited. *J. Geophys. Res.* **109,** E05003 (2004).
27. Aksyuk, A. M. The SiO_2–H_2O system along the lower three-phase curve and approximate values of critical end-point temperature. *Eur. J. Mineral* **9,** 975–986 (1997).
28. Murchie, S. *et al.* Compact reconnaissance imaging spectrometer for Mars (CRISM) on Mars reconnaissance orbiter (MRO). *J. Geophys. Res.* **112,** E05S03 (2007).
29. Malin, M. *et al.* Context camera investigation on board the Mars Reconnaissance Orbiter. *J. Geophys. Res.* **112,** E05S04 (2007).
30. Christensen, P. R., Gorelick, N. S., Mehall, G. L. & Murry, K. C. THEMIS Public Data Releases, Planetary System node, Arizona State University, http://themis-data.asu.edu.

Acknowledgements

This work is supported by the CRISM investigation on MRO under contract from JPL. Thanks to the MRO team for data collection, I. Spitale for HiRISE targeting, and S. Ruff, M. Rice, D. Morris and K. Seelos for discussion and analysis help.

Author contributions

J.R.S. initiated the study, conducted the analysis and wrote manuscript. J.F.M. provided guidance, improved analysis and defined the focus of the work. B.L.E. contributed significantly to the analysis and manuscript contributions. R.E.M. provided research background and technique guidance. S.L.M. was responsible for data acquisition and manuscript refinement.

Additional information

The authors declare no competing financial interests. Reprints and permissions information is available online at http://npg.nature.com/reprintsandpermissions. Correspondence and requests for materials should be addressed to J.R.S.